

**IMPROVED LOCAL LINE BINARY PATTERN
(ILLBP): AN IMPROVED LBP-BASED BIOMETRIC
DESCRIPTOR FOR FACE AND FINGER VEIN
RECOGNITION**

CHAI WUH SHING

UNIVERSITI SAINS MALAYSIA

2013

**IMPROVED LOCAL LINE BINARY PATTERN
(ILLBP): AN IMPROVED LBP-BASED BIOMETRIC
DESCRIPTOR FOR FACE AND FINGER VEIN
RECOGNITION**

by

CHAI WUH SHING

**Thesis submitted in fulfilment of the requirements
for the degree of
Master of Science**

July 2013

ACKNOWLEDGEMENTS

The writing of this dissertation has been one of the most significant academic challenges I have ever had to face. Without the patience, support and guidance of the following people, this research project would not have been completed. It is to them that I owe my deepest gratitude.

First of all, I would like to thank Universiti Sains Malaysia and School of Electrical and Electronic Engineering for providing me this postgraduate project and sponsor me to implement my research project, letting me to gain exposure regarding to the designation of this research project that I am going to cope with in the future.

I wish to express my gratitude to my supervisor, Dr. Hj. Shahrel Azmin who undertook to act as my supervisor despite his many other academic and professional commitments. His wisdom, knowledge and commitment to the highest standards inspired and motivated me. This study would not have been successful without the offer of his invaluable assistance, support and guidance.

I am grateful to my second supervisor Dr. Bakhtiar Affendi Rosdi for his warmth, contribution, helpful comments and responsiveness. He is providing me invaluable advice throughout the duration of my research project implementation.

Furthermore, I would like to give my special thanks to the technician Mr. Jamaludin Bin Mohamad for his patience and willingness to impart his knowledge and to share his experience with me.

Special thanks also to my friends and colleagues, Mr. Waled Hussein Mohammed Al-Arashi, Mr. Yeong Chee Yan and Mr. Yew Chuu Tian for sharing the literature and invaluable assistance. Thank you for all the support and guidelines.

Next, I would like to thank Universiti Sains Malaysia Research University Grant No. 1001/PELECT/814116 and Short Term Grant No. 304/PELECT/6039021 for supporting our finger vein recognition research.

Last but not least, I wish to express my love and gratitude to my beloved families for their understanding and endless love, through the duration of my studies.

Finally, I apologize if there is someone to be missed out. I appreciate everyone involved that bring success to this research project. Thank you very much!

TABLE OF CONTENTS

Acknowledgements	ii
Table of Contents	iv
List of Tables	vii
List of Figures	viii
List of Abbreviations	xii
Abstrak	xiv
Abstract	xvi
CHAPTER 1 – INTRODUCTION	
1.1 Overview	1
1.2 Problem Statement	6
1.3 Objective	7
1.4 Scope	8
1.5 Outline of Thesis	9
CHAPTER 2 – LITERATURE REVIEW	
2.1 Background	10
2.2 Local Binary Pattern.....	12
2.3 Improved Local Binary Pattern	13
2.4 Multi-scale Block Local Binary Pattern	14
2.5 Center Symmetric Local Binary Pattern.....	15
2.6 Direction Local Binary Pattern	15
2.7 Improved Direction Local Binary Pattern	16
2.8 Local Derivative Pattern.....	17
2.9 Local Directional Pattern.....	19
2.10 Local Ternary Pattern.....	21

2.11	Local Line Binary Pattern	22
2.12	Summary	24

CHAPTER 3 – IMPROVED LOCAL LINE BINARY PATTERN

3.1	Introduction	25
3.2	Experiment Setup for Face Recognition	28
3.2.1	Face Image Database	29
3.2.2	Optimum Face Size	31
3.2.3	Classifier	31
3.3	Experiment Setup for Finger Vein Recognition	33
3.3.1	Finger Vein Image Acquisition	33
3.3.2	Finger Vein Image Database	34
3.3.3	Preprocessing	35
3.3.4	Matching	38
3.4	Summary	39

CHAPTER 4 – RESULTS AND DISCUSSIONS

4.1	ILLBP in Face Recognition	40
4.1.1	Determination of Parameters	40
4.1.2	Results Compared with Other Techniques	42
4.1.3	Number of Patterns	44
4.1.4	Analysis of Computational Time	47
4.2	ILLBP in Finger Vein Verification	47
4.2.1	Experimental Results	47
4.2.2	Determination of Parameters	48
4.2.3	Verification Results	53
4.2.4	Speed and Memory	55
4.3	ILLBP analysis	56

CHAPTER 5 – CONCLUSION

5.1	Conclusion	60
5.2	Future Work.....	61
	References	63
	APPENDICES.....	67
	APPENDIX A – CONVERTING RAW IMAGE TO LBP IMAGE	68
	APPENDIX B – TRAINING FACE IMAGES	70
	APPENDIX C – EXAMPLE IMAGES OF A SINGLE INDIVIDUAL IN FRONTAL POSE	72
	APPENDIX D – BAD AND CORRUPTED IMAGES	73
D.1	Bad Images	73
D.2	Corrupted Images.....	75
	APPENDIX E – COMPARISON BETWEEN BEST ILLBP AND LLBP	76
	APPENDIX F – FACE RECOGNITION RATES ACHIEVED BY LOCAL TERNARY PATTERN USING DIFFERENT PARAMETER t ...	77
	APPENDIX G – EXAMPLE OF TRAINING FACE IMAGES PROCESSED BY DIFFERENT DESCRIPTORS	78
	APPENDIX H – EXAMPLE OF CROPPED FINGER VEIN IMAGES.....	90
	APPENDIX I – EXAMPLE OF ENHANCED FINGER VEIN IMAGES.....	93
	List of Publications	95

LIST OF TABLES

		Page
Table 3.1	Five Data Sets of Images Divided According to the Angle the Light Source Direction Makes with the Camera Axis	31
Table 3.2	Comparative Recognition Rates Using Different Face Size	31
Table 3.3	Values of Variables a and b for Different Size (S) of Filtering Mask	38
Table 4.1	Evaluation of Different Parameter Settings	41
Table 4.2	Comparative Recognition Rates Using PCA-kNN	44
Table 4.3	Comparative Recognition Rates Using Multiclass SVM	44
Table 4.4	Determination of Possible Values for ILLBP with parameter $P = 2$	45
Table 4.5	Number of Patterns for ILLBP Descriptor with Different Value of P	46
Table 4.6	Comparative Average Computational Time for Each Technique.	47
Table 4.7	EERs (%) by varying N and S for LLBP based on a sub-dataset of finger vein images.	49
Table 4.8	EERs (%) by varying N and S for $LLBP_v$ based on a sub-dataset of finger vein images.	49
Table 4.9	EERs (%) by varying N , P and S for ILLBP based on a sub-dataset of finger vein images.	50
Table 4.10	EERs (%) by varying N , P and S for $ILLBP_v$ based on a sub-dataset of finger vein images.	50
Table 4.11	Comparison of processing time and binary code length.	56
Table E.1	The best recognition rates achieved by LLBP and ILLBP using PCA-NN with different parameter N	76
Table E.2	The best recognition rates achieved by LLBP and ILLBP using Multiclass SVM with different parameter N	76
Table F.1	PCA-NN	77
Table F.2	Multiclass SVM	77

LIST OF FIGURES

		Page
Figure 1.1	Distributions of the client and the impostor (SYRIS Technology Corp., 2004).	2
Figure 1.2	Illustration of false acceptance, false rejection and equal error rates (SYRIS Technology Corp., 2004).	2
Figure 2.1	The basic LBP descriptor.	13
Figure 2.2	The ILBP descriptor.	13
Figure 2.3	The 9x9 MBLBP operator. In each sub-region, average sum of image intensity is computed. These average sums are then thresholded by that of the center block. MBLBP is then obtained.	14
Figure 2.4	The illustration of CS-LBP, D-LBP, and ID-LBP features for a neighborhood of eight pixels.	17
Figure 2.5	Eight adjacent pixels around I_c .	18
Figure 2.6	Illustration of Kirsch edge masks in all eight directions.	20
Figure 2.7	8-directional edge response positions.	21
Figure 2.8	LDiP code with $k = 3$.	21
Figure 2.9	Illustration of the LTP descriptor with parameter $t = 5$.	22
Figure 2.10	Splitting of an LTP code into positive and negative LBP codes.	23
Figure 2.11	The LLBP descriptor.	24
Figure 3.1	Horizontal component of: (a) $ILLBP_{9,8}$, (b) $ILLBP_{9,4}$, (c) $ILLBP_{9,2}$, (d) $ILLBP_{11,10}$, (e) $ILLBP_{11,4}$, (f) $ILLBP_{11,2}$.	26
Figure 3.2	The ILLBP descriptor.	27
Figure 3.3	Example of face image processed by: (a) original image, (b) $ILLBP_{17,16}$, (c) $ILLBP_{17,8}$, (d) $ILLBP_{17,6}$, (e) $ILLBP_{17,4}$, and (f) $ILLBP_{17,2}$.	27
Figure 3.4	Flow chart of the PCA approach for face recognition.	28
Figure 3.5	Flow chart of the multiclass SVM approach for face recognition.	29

Figure 3.6	Example face images of one of the subjects under different illumination conditions.	30
Figure 3.7	Example of : a) corrupted image, (b) bad image.	30
Figure 3.8	Block diagram of the proposed method.	33
Figure 3.9	Finger vein image capturing device.	34
Figure 3.10	Examples of the captured finger vein images.	35
Figure 3.11	Example of (a) the captured images, (b) the binarized images with the center of the objects and (c) the cropped images for a finger at intervals.	37
Figure 3.12	The resized (top) and their enhanced images.	38
Figure 4.1	Comparison between best ILLBP and LLBP.	42
Figure 4.2	Example face images processed by various descriptors.	43
Figure 4.3	Global histogram for: (a) Fig. 3.3(e), (b) Fig. 3.3(f).	46
Figure 4.4	Histogram extraction using ILLBP description with $P = 2$.	46
Figure 4.5	EERs (%) by varying S for LBP (8, 1) based on a sub-dataset of finger vein images.	51
Figure 4.6	EERs (%) by varying S for LBP (8, 2) based on a sub-dataset of finger vein images.	51
Figure 4.7	EERs (%) by varying S for LDP based on a sub-dataset of finger vein images.	52
Figure 4.8	EERs (%) by varying S for LDiP based on a sub-dataset of finger vein images.	52
Figure 4.9	EERs (%) by varying S for LTP based on a sub-dataset of finger vein images.	53
Figure 4.10	EERs (%) according to various descriptors based on the whole dataset of finger vein images.	54
Figure 4.11	Example of the cropped images and the images after processed by various texture descriptors.	55
Figure 4.12	Illustration of face region processed by ILLBP and LLBP descriptors with: (a) overexposed or underexposed condition (e.g. flat region, edge and corner), (b) image noise.	58

Figure 4.13	Red rectangles show the different outcomes of enhanced finger vein region for: (a) 8th and 9th finger vein images of Figure I.1, (b) 6th and 8th finger vein images of Figure I.2.	58
Figure 4.14	Illustration of enhanced finger vein region processed by ILLBP and LLBP descriptors for Figure 4.13(a). Sub-figures (a) and (c) are part of region inside red rectangle area of the left image of Figure 4.13(a). Sub-figures (b) and (d) are part of region inside red rectangle area of the right image of Figure 4.13(a).	59
Figure 4.15	Illustration of enhanced finger vein region processed by ILLBP and LLBP descriptors for Figure 4.13(b). Sub-figures (a) and (c) are part of region inside red rectangle area of the left image of Figure 4.13(b). Sub-figures (b) and (d) are part of region inside red rectangle area of the right image of Figure 4.13(b).	59
Figure A.1	Example face images processed by LBP descriptor.	68
Figure A.2	The grayscale values of input raw image.	68
Figure A.3	The grayscale values of output LBP image.	69
Figure B.1	The 10 individuals in the Yale Face Database B.	70
Figure B.2	The 28 individuals in the Extended Yale Face Database B.	71
Figure C.1	Example images of a single individual in frontal pose from the Yale Face Database B showing the variability due to illumination.	72
Figure D.1	Bad images.	73
Figure D.1	Bad images (cont).	74
Figure D.2	Corrupted images.	75
Figure G.1	The 38 raw training face images.	78
Figure G.2	38 training face images processed by <i>LBP</i> descriptor.	79
Figure G.3	38 training face images processed by <i>ILBP</i> descriptor.	80
Figure G.4	38 training face images processed by <i>MBLBP</i> descriptor.	81
Figure G.5	38 training face images processed by $CS - LBP_{2,8,0.01}$ descriptor.	82
Figure G.6	38 training face images processed by $D - LBP$ descriptor.	83
Figure G.7	38 training face images processed by $ID - LBP$ descriptor.	84

Figure G.8	38 training face images processed by $LDiP(k = 11)$ descriptor.	85
Figure G.9	38 training face images processed by LDP descriptor.	86
Figure G.10	38 training face images processed by $LTP(t= 11)$ descriptor.	87
Figure G.11	38 training face images processed by $LLBP(N=17)$ descriptor.	88
Figure G.12	38 training face images processed by $ILLBP_{15,2}$ descriptor.	89
Figure H.1	The cropped left middle finger vein images of the 1st subject.	90
Figure H.2	The cropped left index finger vein images of the 26th subject.	91
Figure H.3	The cropped right index finger vein images of the 51th subject.	92
Figure I.1	The cropped and enhanced left index finger vein images of the 3th subject.	93
Figure I.2	The cropped and enhanced right index finger vein images of the 5th subject.	94

LIST OF ABBREVIATIONS

CS-LBP Center Symmetric Local Binary Pattern

D-LBP Direction Local Binary Pattern

EER Equal Error Rate

FAR False Acceptance Rate

FRR False Rejection Rate

GAR Genuine Acceptance Rate

HD Hamming Distance

ICA Independent Component Analysis

ID-LBP Improved Direction Local Binary Pattern

IR Infra-red

ILLBP Improved Local Line Binary Pattern

LBP Local Binary Pattern

LDA Linear Discrimination Analysis

LDiP Local Directional Pattern

LDP Local Derivative Pattern

LLBP Local Line Binary Pattern

MBLBP Multi-scale Block Local Binary Pattern

NN Nearest Neighbor

PCA Principle Component Analysis

ROC Receiver Operating Characteristic

SVM Support Vector Machine

PENAMBAHBAIKAN CORAK PERDUAAN GARIS TEMPATAN (ILLBP): PENAMBAHBAIKAN DESKRIPTOR BIOMETRIK YANG BERASASKAN LBP UNTUK PENGECEMAN MUKA DAN URAT JARI

ABSTRAK

Pengecaman muka di bawah cahaya yang berbeza masih merupakan masalah yang men-
cabar. Perbezaan perubahan cahaya antara imej-imej muka yang sama adalah lebih besar
daripada perbezaan yang disebabkan identiti muka yang tidak sama. Untuk pengecaman
urat jari, kualiti imej urat jari yang rendah akan menyebabkan kadar pengecaman yang
rendah. Ini adalah disebabkan oleh imej urat jari yang tidak jelas dan mempunyai teduhan
yang tidak teratur. Untuk menyelesaikan masalah-masalah ini, telah dicadangkan satu
teknik yang berasaskan teori mudah dan cekap, iaitu deskriptor Penambahbaikan Corak
Perduaan Garis Tempatan (ILLBP) untuk pengecaman muka dan urat jari. Keberkesanan
teknik yang dicadangkan ditunjukkan secara empirikal menggunakan pengelas Analisis
Komponen Prinsipal- k-Jiran Terdekat (PCA-kNN), Mesin Vektor Sokongan Berbilang
Kelas (SVM Berbilang Kelas) dan Jarak Hamming (HD). Perbandingan diberikan di an-
tara varian Corak Perduaan Tempatan (LBP) lain yang sedia ada pada Pangkalan Data
Muka Yale B, Pangkalan Data Muka Yale B Lanjutan dan pangkalan data urat jari kami
sendiri. Kelebihan teknik kami termasuk kadar pengecaman yang lebih tinggi berbanding
dengan varian LBP lain dan masa pengiraan yang cepat. Keputusan eksperimen dengan
menggunakan PCA-kNN sebagai pengelas untuk pengecaman muka menunjukkan ba-
hawa ILLBP terbaik ($N = 15, P = 2$) mencapai kadar pengecaman yang tinggi (89.24%)
dan hanya sedikit lebih rendah daripada LLBP terbaik dengan $N = 17$ (89.36 %). Di

samping itu, ILLBP terbaik ($N = 15$, $P = 2$) mencapai kadar pengecaman yang lebih tinggi (90.97%) dan mengatasi LLBP terbaik dengan $N = 17$ (90.88%) apabila SVM Berbilang Kelas digunakan sebagai pengelas. Selain daripada itu, deskriptor ILLBP menunjukkan kadar EER terendah dalam pengesanan urat jari berbanding dengan deskriptor-deskriptor lain, EER untuk ILLBP dan $ILLBP_v$ (komponen menegak) masing-masing adalah 3.141% dan 2.898%.

IMPROVED LOCAL LINE BINARY PATTERN (ILLBP): AN IMPROVED LBP-BASED BIOMETRIC DESCRIPTOR FOR FACE AND FINGER VEIN RECOGNITION

ABSTRACT

Face recognition under different illumination remains a challenging problem. The variations between the images of the same face due to illuminations are almost always being larger than image variations due to changes in face identity. For finger vein recognition, the recognition rate may be degraded due to low quality of finger vein images. This is because finger vein images are not always clear and can display irregular shadings. A theoretically simple, yet efficient technique, called Improved Local Line Binary Pattern (ILLBP) has been proposed in order to solve the problems. The descriptor can be used for both face and finger vein recognition. The effectiveness of the proposed technique is empirically demonstrated using Principal Component Analysis-k-Nearest Neighbor (PCA-kNN), Multiclass Support Vector Machine (Multiclass SVM) and Hamming Distance(HD) as the classifiers. Comparisons among other existing Local Binary Pattern (LBP) variants on the Yale Face Database B, Extended Yale Face Database B and our own finger vein database have been conducted. The advantages of our technique include higher accuracy compared to other LBP variants and fast computational time. The experimental results for face recognition showed that by using PCA-kNN, the best ILLBP ($N = 15$, $P = 2$) achieved a high recognition rate (89.24%) only slightly worse than the best LLBP with $N = 17$ (89.36%). On the other hand, the best ILLBP ($N = 15$, $P = 2$) achieved a higher recognition rate (90.97%) and outperformed the best LLBP with $N = 17$ (90.88%)

when Multiclass SVM is used as the classifier. Apart from this ILLBP descriptor also has shown lowest EER rate in finger vein verification compared to other descriptors, which are 3.141% and 2.898% for ILLBP and $ILLBP_v$ (vertical component), respectively.

CHAPTER 1

INTRODUCTION

1.1 Overview

Biometrics or biometric recognition is the science and technology of automatically recognizing people by their human body characteristics or traits. In information technology, biometrics refers to the practice of measuring and analyzing human biological data, such as DNA, palm print, fingerprint, eye retina and iris, finger vein, voice pattern, facial pattern and hand geometry, for recognition purposes. Each type has its pros and cons and each one is suited to specific types of applications.

In this research project, scores are used to measure the similarity between a pattern and a template. The higher the score is, the more similar they are. Theoretically, client scores should always be higher than the impostor scores. If this were true, a single threshold that separates the two groups of scores could be used to differentiate between clients and impostors. Unfortunately, due to several reasons, this assumption is not the reality for real world biometric systems. For that reason, no matter how good the classification threshold that is chosen, some classification errors occur (SYRIS Technology Corp., 2004). Basically, there are two types of classification errors: the false acceptance rate (FAR) and the false rejection rate (FRR). A FAR is the measure of probability that a non-matching pair of biometric data is incorrectly accepted as a match by the system. A FRR is the measure of probability that a matching pair of biometric data is incorrectly rejected by the system. The point at which they are both equal is the equal error rate (EER). The choice of thresh-

old becomes a problem if the distributions of client scores and impostor scores overlap, as shown in Figure 1.1. Figure 1.2 illustrates the corresponding FAR, FRR, and EER. A good biometric verification system must have very low FAR and FRR but getting close to zero error rates for both FAR and FRR at the same time are impossible. The FAR error can be close to zero by setting a significantly high threshold. On the other hand, the FRR rate can be close to zero by setting a significantly low threshold. Setting the operating point for the threshold to meet EER is a good idea, this is because it is a balance point between FAR and FRR (SYRIS Technology Corp., 2004).

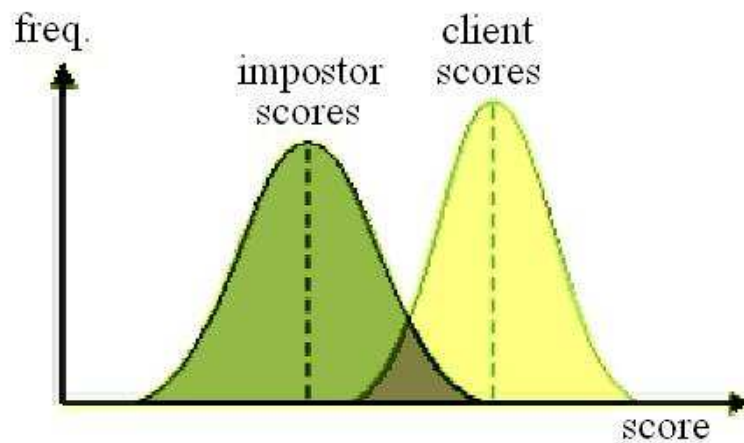


Figure 1.1: Distributions of the client and the impostor (SYRIS Technology Corp., 2004).

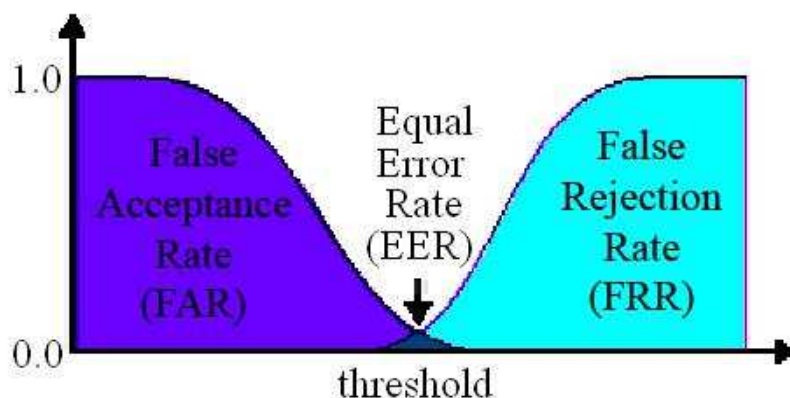


Figure 1.2: Illustration of false acceptance, false rejection and equal error rates (SYRIS Technology Corp., 2004).

In this research project, the main research efforts are devoted to face and finger vein recognition. The main reasons for choosing face recognition because it is good for non-intrusive identity recognition and it can be non-cooperative biometric technique. On the other hand, finger vein recognition is chosen because finger vein is hard to be replicated and the quality of image not easily influenced by skin conditions. In general, the existing approaches to face recognition can be divided into two broad categories: appearance-based and feature-based (Brunelli and Poggio, 1993). The feature-based technique uses geometrical facial features and their geometric relationships, for example elastic active appearance model (Edwards et al., 1998), and elastic graph matching (Wiskott et al., 1997). The appearance-based technique uses holistic information (using whole face) as input to the recognition system. This technique can be induced into the subspace projection step followed by a nearest-neighbor classifier. The purpose of using the subspace projection step is to find a low-dimensional subspace because face image data has the property of high dimension and it is unreasonable to work in this high dimensional space. Some well-known subspace projection techniques are Principal Component Analysis (PCA) (Turk and Pentland, 1991; Turk, 2001), Linear Discriminant Analysis (LDA) (Belhumeur et al., 1997; Martinez and Kak, 2001), and Independent Component Analysis (ICA) (Bartlett et al., 2002). However, the need to further develop robust face recognition techniques to meet real-world situations is still an open research challenge. Some of these challenges are posed by the problems caused by variations in illumination, facial expression, aging, make-up, hair style, pose variation, occlusion, background variation and low resolution images. It is known that lighting changes impose a greater impact on image variation than different personal identities (Moses et al., 1994; Phillips et al., 1998; Zhao et al., 2003; Kim and Kittler, 2005; Heusch et al., 2005). Thus this research project is mainly focused on the problem of compensating for the changes of illumination conditions.

Recently, Local Binary Pattern (LBP) (Ojala et al., 1996) has become a popular technique for face representation due to it is invariant to monotonic gray-scale transformations. Besides LBP, a number of LBP variants have been proposed so far. One of the variants called Improved Local Binary Pattern (ILBP) has been proposed by Jin et al. (2004), the authors considered the effect of the central pixel by assigning the largest weight to the central pixel in order to get all the representations of LBP. Multi-scale Block Local Binary Pattern (MBLBP) is introduced as an extension to the basic LBP due to the LBP operators being too local to be robust (Liao et al., 2007). In MBLBP, the comparison operator between single pixels in LBP is simply replaced with comparison between average gray-values of square blocks. The LBP operator produces rather long histograms and is therefore difficult to use in the context of a region descriptor. To produce more compact binary patterns, Heikkilä et al. (2009), Xiaosheng and Junding (2009) and Junding et al. (2010) introduced Center Symmetric Local Binary Pattern (CS-LBP), Direction LBP (D-LBP) and Improved D-LBP (ID-LBP), respectively for description of interest regions. Three of them compare only 4 pairs of center-symmetric pixels, thus the coding number has been reduced significantly. Recently, Zhang et al. (2010) proposed a high-order local pattern descriptor called Local Derivative Pattern (LDP) for face recognition. The LDP templates extract high-order local information by encoding various distinctive spatial relationships contained in a given local region. Another variant has been proposed by Jabid et al. (2010) to overcome the drawbacks of LBP and is more robust in recognizing face. This technique, called Local Directional Pattern (LDiP) produced its LDiP feature by computing the edge response values in all eight directions at each pixel position and generating a code from the relative strength magnitude. Tan and Triggs (2010) introduced Local Ternary Patterns (LTP), a local texture descriptor that is more discriminant and less sensitive to noise in uniform regions. LTP used three-value encoding instead of two-value

encoding as in the original version of LBP. Petpon and Srisuk (2009) introduced a novel face representation method for face recognition, called Local Line Binary Pattern (LLBP). The basic idea of LLBP is to compute the horizontal and vertical lines binary code separately and its magnitude so that the change in image intensity can be captured. They demonstrated that the proposed method can produce higher recognition rates compared to other LBP-based descriptors on two benchmark face databases.

Since a hand contains lots of information and the information is easily retrieved, hand-based biometrics such as fingerprints (Jain et al., 2010) and palm prints (Guo et al., 2009) are the most popular biometric technologies. Using fingerprints is the most mature hand based biometric method and has been used in many applications for years (Jain et al., 2010). However, fingerprint-based biometric systems are vulnerable to forgery because the fingerprints are easily exposed to others. In addition, the condition of the finger's surface such as dryness and sweat can prevent a clear fingerprint pattern from being obtained (Koichi et al., 2004). This can degrade the system's performance. As for biometric systems based on finger knuckle prints (Zhang et al., 2011) and palm prints (Guo et al., 2009), these features are easy to replicate since they are external to the human body. To overcome the limitations of current hand based biometric systems, finger vein recognition has been researched (Miura et al., 2004). Yanagawa et al.(2007) proved that each finger has unique vein patterns so that it can be used in personal verification. Finger vein-based biometric systems have several benefits when compared with other hand-based biometric methods. First, the finger vein pattern is hard to replicate since it is an internal feature. In addition, the quality of the captured vein pattern is not easily influenced by skin conditions. Moreover, as compared with palm vein-based verification systems (Zhang et al., 2007), the size of the device can be made much smaller. Most of the current available approaches for finger vein recognition (Miura et al., 2004; Yu et al., 2009; Song et al., 2011)

have similarities in their feature extraction method which utilizes the features of the segmented blood vessel network for recognition. However, due to optical blurring and skin scattering problems, finger vein images are not always clear and can display irregular shadings (Lee and Park, 2011). Therefore, a new finger recognition method is needed to overcome the issues in this field. To solve the problem, Lee et al.(2011) proposed a method for finger vein recognition LBP and LDP (Zhang et al., 2010). In the proposed method, the captured finger vein images are enhanced by modified Gaussian high-pass filter and then LBP and LDP are applied to extract the binary codes from the enhanced images. Besides LDP, LLBP descriptor has been applied to finger vein recognition and the authors demonstrated a better accuracy than both LBP and LDP (Rosdi et al., 2011).

LLBP have been proven to give better results in both face and finger vein recognition. However, the performance of the LLBP depends heavily on length of local line. Long horizontal and vertical local lines are computationally expensive, both in terms of computing speed and memory consumption. Thus, a novel improved descriptor, called Improved Local Line Binary Pattern (ILLBP) is introduced in this research project. The descriptor is inspired by LLBP due to it characterizing the change in image intensity by using the kernel with a straight line shape. The basic idea of ILLBP is similar to the original LLBP but the main difference is the ILLBP compares the gray value only from a part of pixels with the center pixel, instead of comparing the gray-value of all the pixels on the local line with the center pixel as in LLBP.

1.2 Problem Statement

A general statement of the problem that tried to be solved in this research project can be formulated as follows:

- Face recognition

Facial appearance changes dramatically due to different lighting conditions, including the type of illumination and intensity, and "the variations between the images of the same face due to illuminations almost always being larger than image variations due to changes in face identity" as mentioned in Moses et al. (1994). LLBP descriptor (Petpon and Srisuk, 2009) can cope with this problem but it is computationally expensive when the length of local line is getting longer which resulted in longer processing time.

- Finger vein recognition

Finger vein images are not always clear and can display irregular shadings due to the optical blurring and skin scattering problems. Therefore, segmentation errors can occur during the feature extraction process due to the low quality of finger vein images. When the networks are not segmented properly, the recognition accuracy may be degraded. LLBP descriptor can cope with this problem but it is computationally expensive when the length of local line is getting longer which resulted longer processing time. Apart from this, it needs more memory size to store the binary codes as the extracted binary code length is getting longer.

Hence, an improved LLBP which solves the computational time and memory size with higher accuracy is desired in this research project.

1.3 Objective

The objectives of the research undertaken here are:

1. To develop an improved LBP-based descriptor for face identification which is robust

to illumination changes. The proposed descriptor must achieve higher recognition rate and computationally simpler than other existing LBP-based descriptors.

2. To apply the proposed descriptor in finger vein verification. The proposed descriptor must achieve higher recognition rate and computationally simpler than other existing LBP-based descriptors.
3. To evaluate and compare the proposed descriptor with other existing LBP-based descriptors.

1.4 Scope

This thesis covers the following scope:

1. To show the effectiveness of the proposed method for illumination robust face recognition, experiments were conducted on face images with the fixed pose and same facial expression but different illumination settings.
2. To evaluate the performance of proposed finger vein recognition method, finger vein database which was developed at our lab was used. Each subject provided finger vein images of four fingers, that is left index, left middle, right index and right middle fingers.
3. A special imaging device was utilized to capture and collect finger vein images. To reduce finger alignment problems, especially finger rotation, an open window with a fixed size (2.5 cm x 2.5 cm) was set for the user to place their finger within during the capturing process. The small size of open window helps to solve alignment problems but the limitation is the finger can't fit in the open window properly if it thicker than 2.5 cm.

1.5 Outline of Thesis

The work described in this thesis is organized into five chapters. In Chapter 1, the content provides the reader with a general overview of the biometric system and face and finger vein recognition systems. It also shows the objectives of the research to be achieved as well as the scope of the thesis.

Chapter 2 reviews the major work done previously in LBP-based descriptor research. A literature review of the most-recent LBP-based descriptors is presented. Chapter 3 then describes the methodology of the project. It includes a discussion of the method used in this research project. It also discusses the procedure and processes involved for the software development of the entire project such as the flow of project and program related descriptions. Flow charts and block diagrams are used to show the flow of the process for the system. Chapter 4 exhibits the results and analysis together with a discussion of the overall situation. It also discusses the results obtained from each part of the entire research project. Lastly, a conclusion of the thesis is presented in Chapter 5 which includes recommendations for future study.

CHAPTER 2

LITERATURE REVIEW

2.1 Background

When dealing with biometric technologies, there are two types of matching to consider: identification or verification.

- Verification (1:1)- A one-to-one matching of a biometric for a person whom you wish to verify.
- Identification (1:N)- A one-to-many matching of a biometric against all the existing records stored in the database in an attempt to identify an unknown person.

Biometric verification equates to: "Am I who I claim I am?" For example, when the system enrolls an individual for the first time, the system also captures additional information such as name and personal identification number. When the same individual returns, they are identified through one of those pieces of additional information, then verified through the biometric match. It determined whether the similarity between pattern and template is sufficient to has privileges to perform a certain action. The pattern that is verified only is compared against a previously collected biometric sample from the individual. Verification only proves that the person in front of the system now is the one who originally enrolled. Because of this one-to-one matching, biometric verification systems are, of course, much faster than biometric identification systems. Most of the commercial applications for biometrics such as access control, entrance security or time attendance

use biometric verification.

Biometric identification, on the other hand, answers the question "Who am I?". The system is trained with the patterns of several persons. For each of the persons, a biometric template is computed in this training stage. A pattern that is going to be identified is compared against each available template, generating a score describing the similarity between the pattern and the template. The system assigns the pattern to the person with the most similar biometric template. To prevent impostor patterns from being wrongly accepted by the system, the similarity has to meet or exceed a certain threshold. Otherwise, the pattern is rejected if this minimum level of threshold is not reached. In the identification case, because it needs to match all the existing records stored in the entire database with the new biometric pattern, it can be time consuming and is less commonly used for real-time applications such as entrance security, access control, and time attendance system. Biometric identification is used most frequently in law enforcement agencies and forensics to identify and apprehend criminals.

In the past few years, many approaches have been proposed to cope with illumination variation problems with improvements in face recognition (Chen et al., 2006; Zhang and Samaras, 2006; O'Toole et al., 2007; Shao and Wang, 2009; Wang et al., 2009; Tan and Triggs, 2010; Mian, 2011; Bozorgtabar et al., 2012; Farag and Atta, 2012). Recently, Local Binary Pattern (LBP) (Ojala et al., 1996) has become a popular technique for face representation due to it being invariant to monotonic gray-scale transformations. Apart from this, LBP descriptors also were adopted by Lee et al. (2011) for finger vein recognition. Besides LBP, a number of LBP variants have been proposed to date. All LBP variants will be discussed in detail in this section.

2.2 Local Binary Pattern

The Local Binary Pattern (LBP) descriptor is a non-parametric 3x3 kernel which summarizes the local spacial structure of an image. The basic idea of the LBP descriptor was originally proposed by Ojala et al. (1996). They demonstrated that LBP can produce higher recognition rates compared to other techniques on nine classes of textures taken from Brodatz's album (Brodatz, 1966). Ahonen et al. (2006) presented an efficient facial image representation based on LBP texture features. Their research showed the simplicity of LBP-based face representation extraction and its robustness with respect to facial expression, aging, illumination and alignment. Furthermore, LBP not only applied to face recognition, Lee et al. (2011) proposed a method for finger vein recognition using LBP.

LBP is used to threshold each of the eight surrounding pixels in a circular region with the intensity of the central pixel (Figure 2.1). The basic LBP encodes 256 simple feature detectors in a single 3x3 descriptor. During the LBP operation, the value of the LBP code of a pixel (x_c, y_c) is given in Equation (2.1) where g_c corresponds to the gray value of the center pixel (x_c, y_c) , g_i refers to gray values of 8 equally spaced pixels, and $s(\cdot)$ function defines a thresholding function as in Equation (2.2). Hence, a local binary pattern is obtained by first concatenating these binary numbers and then converting the sequence into a decimal representation. Each pixel in raw image need to be processed by LBP descriptor in order to get the LBP image (refer to Appendix A).

$$LBP(x_c, y_c) = \sum_{i=0}^7 s(g_i - g_c) \cdot 2^i \quad (2.1)$$

$$s(x) = \begin{cases} 1, & x \geq 0, \\ 0, & x < 0. \end{cases} \quad (2.2)$$

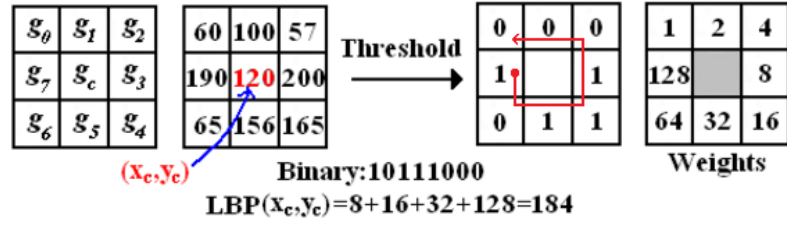


Figure 2.1: The basic LBP descriptor.

2.3 Improved Local Binary Pattern

Jin et al. (2004) presented a face detection approach using Improved Local Binary Patterns (ILBP) as facial representation. They suggested considering the effect of the central pixel in order to get all the representations of LBP. They assigned the largest weight to the central pixel due to it always providing more information than its neighboring pixel (Figure 2.2). The ILBP of a given pixel can be expressed as follows:

$$ILBP(x_c, y_c) = \sum_{i=0}^8 s(g_i - m) \cdot 2^i \quad (2.3)$$

where m corresponds to the mean gray value of all the pixels in the 3x3 kernel, and $s(\cdot)$ function is the same as in Equation (2.2). The decimal result of 9 bits can then generate $2^9 - 1 = 511$ unique values instead of $2^8 = 256$ LBP codes. The total number of unique values is 511 and not 512 because of it being impossible to get all nine pixels at the same time to have values which are smaller than the mean value.

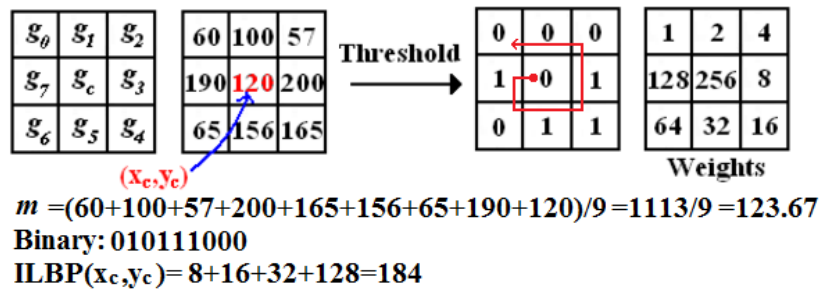


Figure 2.2: The ILBP descriptor.

2.4 Multi-scale Block Local Binary Pattern

Liao et al. (2007) introduced Multi-scale Block Local Binary Pattern (MBLBP) as an extension to the basic LBP due to it provides a more complete image representation by encoding not only microstructures but also macrostructures of image patterns. Their experiments showed that the MBLBP method significantly outperforms other LBP based face recognition algorithms. In MBLBP, the comparison descriptor between single pixels in LBP is simply replaced by a comparison between average gray-values of square blocks (Figure 2.3. The size of the kernel can be 3x3, 9x9, 15x15 and so on (3x3 MBLBP is equivalent to original LBP). An output value of the MBLBP descriptor can be obtained as follows:

$$MBLBP(x,y) = \sum_{i=0}^7 s(g_i - g_c) \cdot 2^i \quad (2.4)$$

where g_c is the average gray-value obtained at central block and g_i is the average gray-value obtained at its neighboring block, and $s(\cdot)$ function is the same as in Equation (2.2).

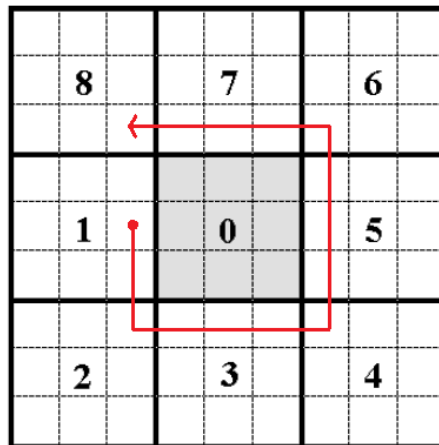


Figure 2.3: The 9x9 MBLBP operator. In each sub-region, average sum of image intensity is computed. These average sums are then thresholded by that of the center block. MBLBP is then obtained.

2.5 Center Symmetric Local Binary Pattern

Heikkilä et al. (2009) presented a Center Symmetric Local Binary Pattern (CS-LBP) modification for the description of interest regions. In the matching and object category classification experiments, their descriptor outperformed the Scale-Invariant Feature Transform (SIFT) descriptor (Lowe, 2004). Furthermore, the CS-LBP descriptor is computationally simpler than the SIFT descriptor. The CS-LBP is an effective extension because it produces more compact version of binary patterns where only 4 pairs of center-symmetric pixels are compared, thus the coding number is reduced significantly; see Figure 2.4. For a eight-neighborhood of a pixel, LBP produces 256 (2^8) different binary patterns while CS-LBP only produces 16 (2^4) different binary patterns. The scheme function of CS-LBP is given as

$$CS_LBP_{R,N,T}(x,y) = \sum_{i=0}^{\frac{N}{2}-1} s_{CS_LBP}(p_i, p_{i+\frac{N}{2}}) \cdot 2^i \quad (2.5)$$

where p_i and $p_{i+\frac{N}{2}}$ are the gray-level of center-symmetric pairs of pixels on a circle of radius R with N equally spaced pixels, T is the threshold used to fine-tune the robustness of the flat region, and the $s(\cdot)$ function is expressed as:

$$s_{CS_LBP}(p_i, p_{i+\frac{N}{2}}) = \begin{cases} 1, & p_i - p_{i+\frac{N}{2}} > T, \\ 0, & \text{otherwise.} \end{cases} \quad (2.6)$$

2.6 Direction Local Binary Pattern

One of the drawbacks of the CS-LBP descriptor is that it discards important information because of the ignorance of the center pixel. Furthermore, it is also difficult to choose a suitable threshold. Therefore, Xiaosheng and Junding (2009) proposed an improved CS-

LBP, called Direction LBP (D-LBP) to cope with this problem. It was evaluated against the LBP and CS-LBP descriptors on three texture databases with different evaluation criteria. The experimental results showed that the D-LBP descriptor is better for most of the test cases than the other two descriptors. The D-LBP descriptor describes the local pattern by considering the relation of the center pixel and the center-symmetric pixels instead of comparing the gray-value between the center symmetric pair of pixels as CS-LBP. The D-LBP can be expressed as follows:

$$D_LBP(x,y) = \sum_{i=0}^3 s_{D_LBP}(p_i, p_c, p_{i+4}) \cdot 2^i \quad (2.7)$$

where p_c , p_i , and p_{i+4} correspond to the gray-level of center pixel and the center-symmetric pairs of pixels. For the $s(\cdot)$ function, it can be expressed as:

$$s_{D_LBP}(p_i, p_c, p_{i+4}) = \begin{cases} 1, & (p_i \geq p_c \ \& \ p_c \geq p_{i+4}) \mid (p_i < p_c \ \& \ p_c < p_{i+4}) \\ 0, & otherwise \end{cases} \quad (2.8)$$

2.7 Improved Direction Local Binary Pattern

The common characteristic of CS-LBP and D-LBP is that only the gray-level difference between the pixels in a local region is considered. It is clear that such techniques are much affected by noise. In order to overcome this problem, an Improved D-LBP (ID-LBP) descriptor was introduced by Junding et al. (2010). They evaluated the ID-LBP against the CSLBP and D-LBP descriptors on two common used image databases in image retrieval. The experimental results showed that the ID-LBP operator is better than D-LBP to some extent for texture images and it is more effective than the other two descriptors for nat-

ural image. ID-LBP describes the local pattern by considering the relation between the local gray mean and the center-symmetric pixels instead of comparing the gray-value between the center-symmetric pixels and the center pixel as D-LBP. The ID-LBP descriptor is mathematically described as:

$$ID_LBP(x,y) = \sum_{i=0}^3 s_{ID_LBP}(p_i, m, p_{i+4}) \cdot 2^i \quad (2.9)$$

$$s_{ID_LBP}(p_i, m, p_{i+4}) = \begin{cases} 1, & (p_i \geq m \ \& \ m \geq p_{i+4}) \mid (p_i < m \ \& \ m < p_{i+4}) \\ 0, & otherwise \end{cases} \quad (2.10)$$

where $m = \frac{1}{8} \sum_{i=1}^8 p_i$. A simple illustration of CS-LBP, D-LBP, and ID-LBP is shown in Figure 2.4 for eight neighbors. Obviously 3 of them produce only 16 (2^4) different binary patterns for eight neighbors.

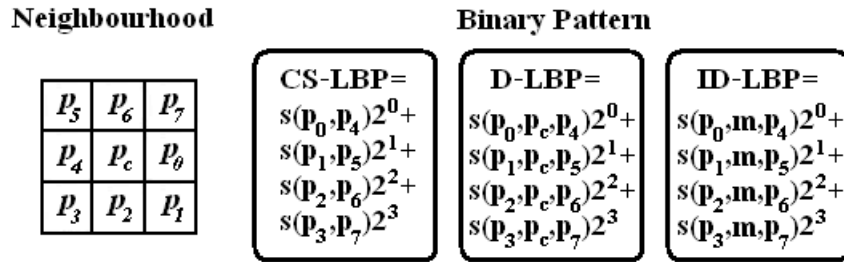


Figure 2.4: The illustration of CS-LBP, D-LBP, and ID-LBP features for a neighborhood of eight pixels.

2.8 Local Derivative Pattern

Zhang et al. (2010) proposed a high-order descriptor, called Local Derivative Pattern (LDP), for face recognition. The n^{th} -order LDP is proposed to encode the $(n - 1)^{th}$ -order derivative information, which can capture more elaborate and detailed discriminative features than the first-order local pattern used in LBP. Their experimental results on five

benchmark face databases show that the high-order LDP consistently performed much better than LBP for both face identification and face verification under various conditions.

In this research, the codes are extracted from a filtered image using a second-order LDP, considering the 0° , 45° , 90° , and 135° directions. If the eight adjacent pixels are positioned around the center position (I_c), as shown in Figure 2.5, the first-order derivative bits along each direction are defined as:

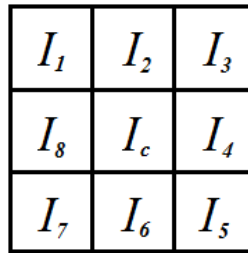


Figure 2.5: Eight adjacent pixels around I_c .

$$\begin{aligned}
 B_{0^\circ}(x_c, y_c) &= f(I_4 - I_c) \\
 B_{45^\circ}(x_c, y_c) &= f(I_3 - I_c) \\
 B_{90^\circ}(x_c, y_c) &= f(I_2 - I_c) \\
 B_{135^\circ}(x_c, y_c) &= f(I_1 - I_c)
 \end{aligned} \tag{2.11}$$

$$f(k) = \begin{cases} 1, & k > th, \\ 0, & k \leq th. \end{cases} \tag{2.12}$$

where (x_c, y_c) and th denote the position of the center pixel I_c and a predefined threshold, respectively. The predefined threshold was set to 0 in this research project. The LDP extracts the feature codes from an exclusive-OR (\otimes) operation of the corresponding first-order derivative bits between the center pixel and eight adjacent pixels. Based on the

above method, LDP features can be generated using the following equations:

$$LDP_{\alpha}(x_c, y_c) = \sum_{i=1}^8 \{B_{\alpha}(x_c, y_c) \otimes B_{\alpha}(x_c + u_i, y_c + v_i)\} \cdot 2^{i-1} \quad (2.13)$$

$$u_a = \begin{cases} -1, & \text{if } a = 1 \\ 0, & \text{if } a = 2 \\ 1, & \text{if } a = 3 \\ 1, & \text{if } a = 4 \\ 1, & \text{if } a = 5 \\ 0, & \text{if } a = 6 \\ -1, & \text{if } a = 7 \\ -1, & \text{if } a = 8 \end{cases} \quad v_a = \begin{cases} -1, & \text{if } a = 1 \\ -1, & \text{if } a = 2 \\ -1, & \text{if } a = 3 \\ 0, & \text{if } a = 4 \\ 1, & \text{if } a = 5 \\ 1, & \text{if } a = 6 \\ 1, & \text{if } a = 7 \\ 0, & \text{if } a = 8 \end{cases} \quad (2.14)$$

$$LDP_{\alpha}(x_c, y_c) = \{LDP_{\alpha}(x_c, y_c) | \alpha = 0^{\circ}, 45^{\circ}, 90^{\circ}, 135^{\circ}\} \quad (2.15)$$

Apart from this, the LDP descriptor also has been adopted by Lee et al. (2011) for finger vein recognition.

2.9 Local Directional Pattern

Jabid et al. (2010) introduced a appearance based-feature descriptor, called Local Directional Pattern (LDiP), for face representation and evaluated its performance in facial expression recognition. Their experimental results validated that the LDiP performed better than LBP in expression recognition. An LDiP feature was obtained by calculating the edge response values in eight different directions at each pixel and encoding them into an 8 bit binary number using the relative strength of these edge responses. For a given central pixel in the image, the eight-directional edge response values $\{m_i\}$, $i=0, 1, \dots, 7$

were computed by Kirsch masks, M_i , in eight different directions centered on the pixel's position. The illustration of Kirsch edge masks is shown in Figure 2.6. The response values are not equally important in all eight directions. The presence of an edge or a corner shows high response values in certain specific directions. Therefore, it is important to know the most prominent k directions to produce the LDiP. Hence, the top k values $|m_j|$ was set to 1 and the remaining $(8 - k)$ bits of the 8-bit LDiP pattern are set to 0. Finally,

$$\begin{array}{cccc}
 \begin{bmatrix} -3 & -3 & 5 \\ -3 & 0 & 5 \\ -3 & -3 & 5 \end{bmatrix} & \begin{bmatrix} -3 & 5 & 5 \\ -3 & 0 & 5 \\ -3 & -3 & -3 \end{bmatrix} & \begin{bmatrix} 5 & 5 & 5 \\ -3 & 0 & -3 \\ -3 & -3 & -3 \end{bmatrix} & \begin{bmatrix} 5 & 5 & -3 \\ 5 & 0 & -3 \\ -3 & -3 & -3 \end{bmatrix} \\
 \text{East } M_0 & \text{North East } M_1 & \text{North } M_2 & \text{North West } M_3 \\
 \begin{bmatrix} 5 & -3 & -3 \\ 5 & 0 & -3 \\ 5 & -3 & -3 \end{bmatrix} & \begin{bmatrix} -3 & -3 & -3 \\ 5 & 0 & -3 \\ 5 & 5 & -3 \end{bmatrix} & \begin{bmatrix} -3 & -3 & -3 \\ -3 & 0 & -3 \\ 5 & 5 & 5 \end{bmatrix} & \begin{bmatrix} -3 & -3 & -3 \\ -3 & 0 & 5 \\ -3 & 5 & 5 \end{bmatrix} \\
 \text{West } M_4 & \text{South West } M_5 & \text{South } M_6 & \text{South East } M_7
 \end{array}$$

Figure 2.6: Illustration of Kirsch edge masks in all eight directions.

the LDiP code is derived by:

$$LDiP_k(x_c, y_c) = \sum_{i=0}^7 b_i(m_i - m_k) \cdot 2^i \quad (2.16)$$

$$b_i(a) = \begin{cases} 1, & a \geq 0, \\ 0, & a < 0. \end{cases} \quad (2.17)$$

where m_k is the k -th most significant directional response. Figure 2.7 shows the LDiP bit positions and Figure 2.8 shows an LDiP encoding procedure with $k=3$.

m_3	m_2	m_1
m_4	X	m_0
m_5	m_6	m_7

Figure 2.7: 8-directional edge response positions.

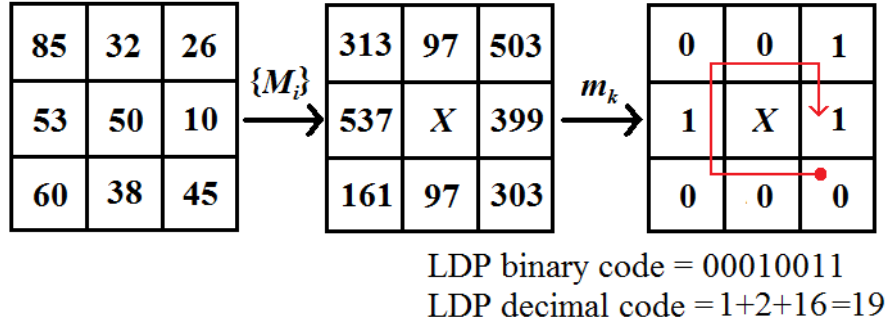


Figure 2.8: LDiP code with $k=3$.

2.10 Local Ternary Pattern

The fact that LBP thresholds the pixels of the neighborhood at exactly the value of the central pixel makes it sensitive to noise in the near-uniform image regions. Since many facial regions such as forehead and cheek are relatively uniform, it is potentially beneficial to improve the performance and robustness of the descriptors in these regions. Hence, Tan and Triggs (2010) presented Local Ternary Pattern (LTP). Their experiments showed that LTP descriptor outperformed several existing preprocessors for a range of feature sets, data sets and lighting conditions. LTP uses three-value encoding instead of two-value encoding as in the original version of LBP, in which gray-levels in a zone of width t around g_c are set to zero, ones above this are set to +1, and ones below it to -1. During the LTP operation, the value of the LTP code of a pixel (x_c, y_c) is given by::

$$LTP(x_c, y_c) = \sum_{i=0}^7 s'(g_i, g_c, t) \cdot 2^i \quad (2.18)$$

where g_c corresponds to the gray value of the center pixel (x_c, y_c) , g_i refers to gray values of 8 equally spaced pixels, t is the predefined threshold set by user, and $s'(\cdot)$ function defines a thresholding function as follows:

$$s'(g_i, g_c, t) = \begin{cases} 1, & g_i \geq g_c + t \\ 0, & |g_i - g_c| < t \\ -1, & g_i \leq g_c - t \end{cases} \quad (2.19)$$

The illustration of LTP descriptor is shown in Figure 2.9 with parameter t equals to 5, so the tolerance interval is $[49, 59]$. For simplicity Tan and Triggs (2010) used a coding scheme that splits each ternary pattern into two separate LBP patterns (positive and negative halves) as illustrated in Figure 2.10 to create a descriptor double the size of LBP.

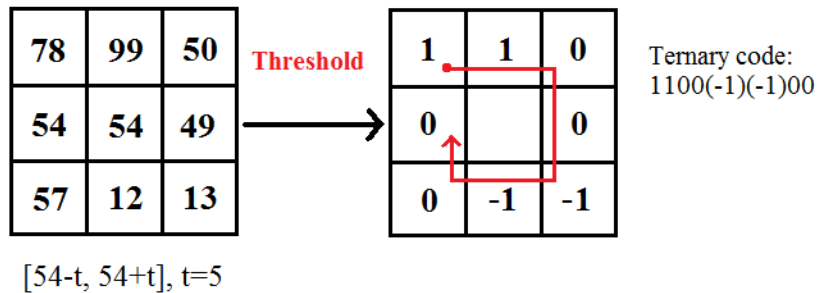


Figure 2.9: Illustration of the LTP descriptor with parameter $t = 5$.

2.11 Local Line Binary Pattern

Petpon and Srisuk (2009) proposed a face representation technique, named Local Line Binary Pattern (LLBP). They demonstrated that LLBP descriptor can produce higher recognition rates compared to LBP on two benchmark face databases. The descriptor consists of 2 components: horizontal component and vertical component. The magnitude of LLBP can be obtained by calculating the line binary codes for both components. The illustration of LLBP descriptor is shown in Figure 2.11 and its mathematical definitions are given in

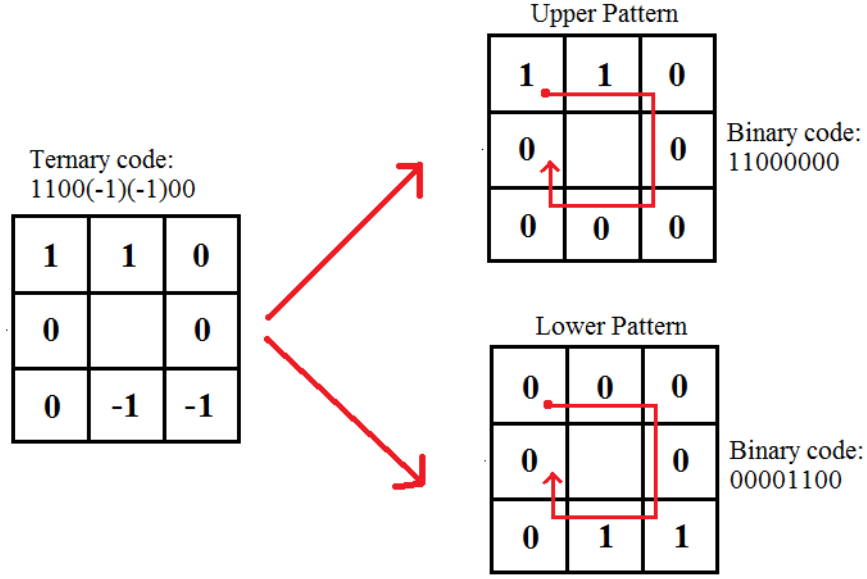


Figure 2.10: Splitting of an LTP code into positive and negative LBP codes.

Equation (2.20) to Equation (2.22). $LLBP_h$, $LLBP_v$ and $LLBP_m$ are LLBP in the horizontal direction, vertical direction, and its magnitude, respectively. N is the length of the line in pixels, h_n represents the pixel intensities along the horizontal line and v_n the pixel intensities along the vertical line, $c = \frac{N}{2}$ is the position of the center pixel h_c on the horizontal line and v_c on the vertical line, and $s(\cdot)$ function is the same as in Equation (2.2). One of the benefits of the LLBP descriptor is it can emphasize the change in image intensity such as vertices, edges and corners.

$$LLBP_{hN,c}(x,y) = \sum_{n=1}^{c-1} s(h_n - h_c) \cdot 2^{c-n-1} + \sum_{n=c+1}^N s(h_n - h_c) \cdot 2^{n-c-1} \quad (2.20)$$

$$LLBP_{vN,c}(x,y) = \sum_{n=1}^{c-1} s(v_n - v_c) \cdot 2^{c-n-1} + \sum_{n=c+1}^N s(v_n - v_c) \cdot 2^{n-c-1} \quad (2.21)$$

$$LLBP_m = \sqrt{LLBP_h^2 + LLBP_v^2} \quad (2.22)$$

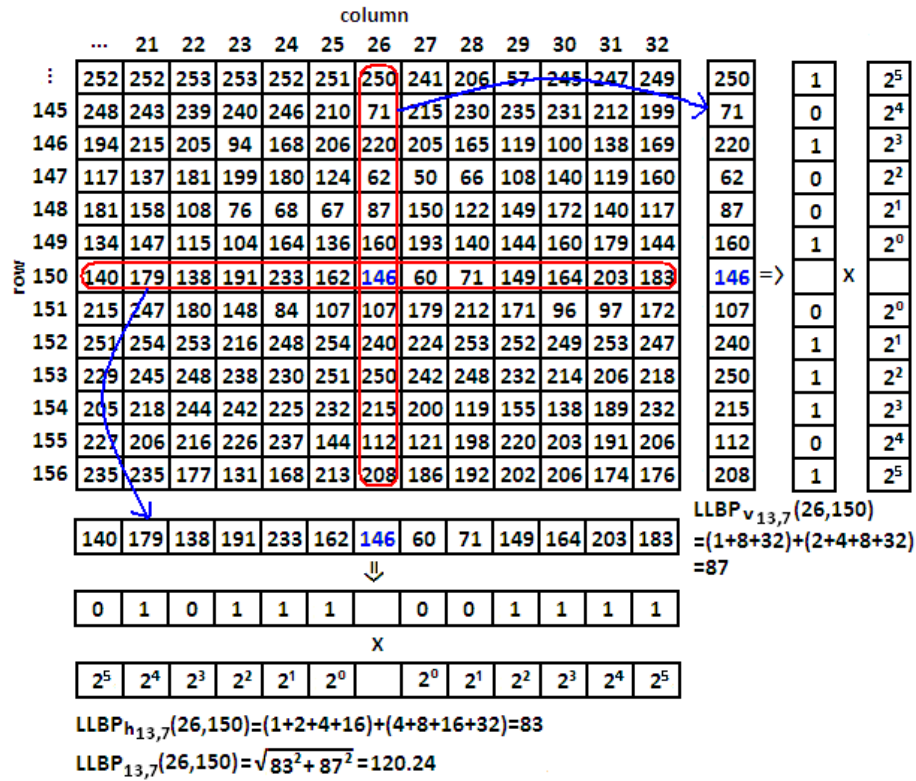


Figure 2.11: The LLBP descriptor.

2.12 Summary

In this chapter, the theoretical concepts of LBP and its variants are discussed in brief. The neighborhood shape for most of the LBP variants is circular/square, except LLBP which is a straight line with a pixel of length N . CS-LBP and LDiP do not involve its center pixel when calculating the binary code. ILBP, MB-LBP and ID-LBP need to compute the mean value before obtaining the binary code. CS-LBP and LTP need to set a suitable threshold value before obtaining the binary code. These LBP variants were selected for comparison in this study. After providing a detailed review of the literature on existing LBP variants in this chapter, this study proposes a new biometric descriptor in Chapter 3. This is found to yield a more accurate outcome.